Pitting Corrosion of 2205 Duplex Stainless Steel at High Concentrations of NaCl Solution

Chuan Liu [1,2], *Min Gong* [1,2,*], *Xingwen Zheng* [2,3]

[1] School of Material and Science Engineering, Sichuan University of Science & Engineering, Zigong 643000, China, Zigong 643000, China
[2] Key Laboratory of Material Corrosion and Protection of Sichuan Province, Zigong 643000, China
[3] School of Chemical and Environmental Engineering, Sichuan University of Science & Engineering, Zigong 643000, China
[*]E-mail: gmsuse@126.com

Critical pitting temperature (CPT) of 2205 duplex stainless steel (2205 DSS) in different concentrations of NaCl solution was investigated through cyclic voltammetry and potentiostatic technique, and the difference of corrosion behavior of 2205 DSS in NaCl solution under high and low CPT was compared. The results revealed that the concentration of NaCl solution has little effect on CPT of 2205 DSS in the range of studied concentrations (50 ~ 300 g/L), and the CPT is between 40 and 45 °C. However, the corrosion current density, electrochemical impedance and corrosion morphology of 2205 DSS were significantly different under temperatures below the CPT and above the CPT.

1. INTRODUCTION

Duplex stainless steel consists of approximately equal volume of austenite phase and ferrite phase, which combines the advantages of both ferrite stainless steel and austenitic stainless steel, therefore, it shows good resistance to pitting corrosion, crevice corrosion and stress corrosion [1-5]. Nowadays, duplex stainless steel has been widely applied in the Oil and gas refining, marine engineering, seawater desalination and vacuum salt [6-10]. However, in aggressive environment, duplex stainless steel still suffers from localized corrosion, especially in the environment containing high chloride concentration at high temperature. It is well known that pitting occurs when stainless steel is immersed in solutions with halide ions concentration exceeding a critical value, with chloride

ion being the most common [11-14]. Peguet et al. [15] studied the critical potential breakdown of duplex stainless steel's passivation films in 0.5 M NaCl aqueous solution at different temperatures. Deng and coworkers [16] investigateed the pitting and repassivation behaviors of duplex stainless steel in 1 M NaCl solution. Jeon et al. [17] elucidated the effects of sulfur addition on pitting corrosion and machinability behavior of super duplex stainless steel containing rare earth metals, the influence of molybdate on critical pitting temperature of 2205 DSS in 0.1 M NaCl solution also has been studied by Eghbali and coworkers [18]. Moreover, the effect of solution heat treatment on the pitting corrosion resistance of 2205 DSS has also been investigated [19-22]. However, few studies have focused on the corrosion behavior of duplex stainless steel in high concentration NaCl solution, but which is the environment that stainless steel has to confront in the process of vacuum salt and seawater desalination. The present work investigated the corrosion behavior of 2205 DSS in different concentrations of NaCl solutions using cyclic voltammeter, potentiostatic technique, potentiodynamic polarization, electrochemical impedance spectroscopy and morphology analysis.

2. EXPERIMENTAL

2.1. Material and Electrolyte

The 2205 DSS used in the experiment is round rod with a diameter of 16 mm, its weight percentage compositions are listed in Table 1. Cylindrical samples cut from the round rod were used as working electrode and morphology analysis. The exposed surface area of working electrode was 2 cm^2, and its remainder was embedded by epoxy. Prior to each experiment, the specimen was wet ground to the 800 # abrasive paper, degreased with acetone, rinsed with distilled water and dried in the air. The NaCl solutions were prepared by the analytical grade NaCl and deionized water.

Table 1. Chemical composition of the used 2205 DSS

Element	C	Cr	Ni	Mo	Mn	S	Fe
wt/%	<0.03	22	5	3.3	2.0	0.03	Bal.

2.2. Electrochemical measurements

The electrochemical measurements were performed using a potentiostat Solartron 1287 and a frequency response analyzer Solartron SI 1260 with a conventional three-electrode cell, which contains a platinum grid, a saturated calomel reference electrode (SCE) and 2205 DSS working electrode. Electrochemical measurements were controlled with Zplot and Corrware software and were analyzed through ZView and CorrView software, respectively. The working electrode was firstly immersed into NaCl solution for 30 min at the beginning of electrochemical testing in order to stabilize the open circuit potential (OCP). The parameters of the cyclic voltammetry were set as follows: the initial potential was -0.2V vs. OCP, the scan rate was 5 mV/s [23] and the limiting current density was 2

mA/cm^2. A polarization potential of 0.2 V vs. SCE was applied to the working electrode in the potentiostatic test, the temperature was changed from 25 °C with the rate of 1±0.2 °C/min until the current density arrived at 0.4 mA/cm^2. The frequency range of electrochemical impedance spectroscopy (EIS) was $10^{-2} \sim 10^5$ Hz and the AC amplitude was 5 mV, while the scanning speed of potentiodynamic polarization was 0.5 mV/s and the scanning range was from -250 mV to +350 mV (vs OCP).

2.3. Morphology Analysis

The surface analysis samples were polished and then immersed in 300 g/L NaCl solution at 70 ℃ for 7 days, thus the surface morphology was examined with VEGA 3SBU scanning electron microscope (SEM).

3. RESULTS AND DISCUSSION

3.1 Cyclic voltammetry
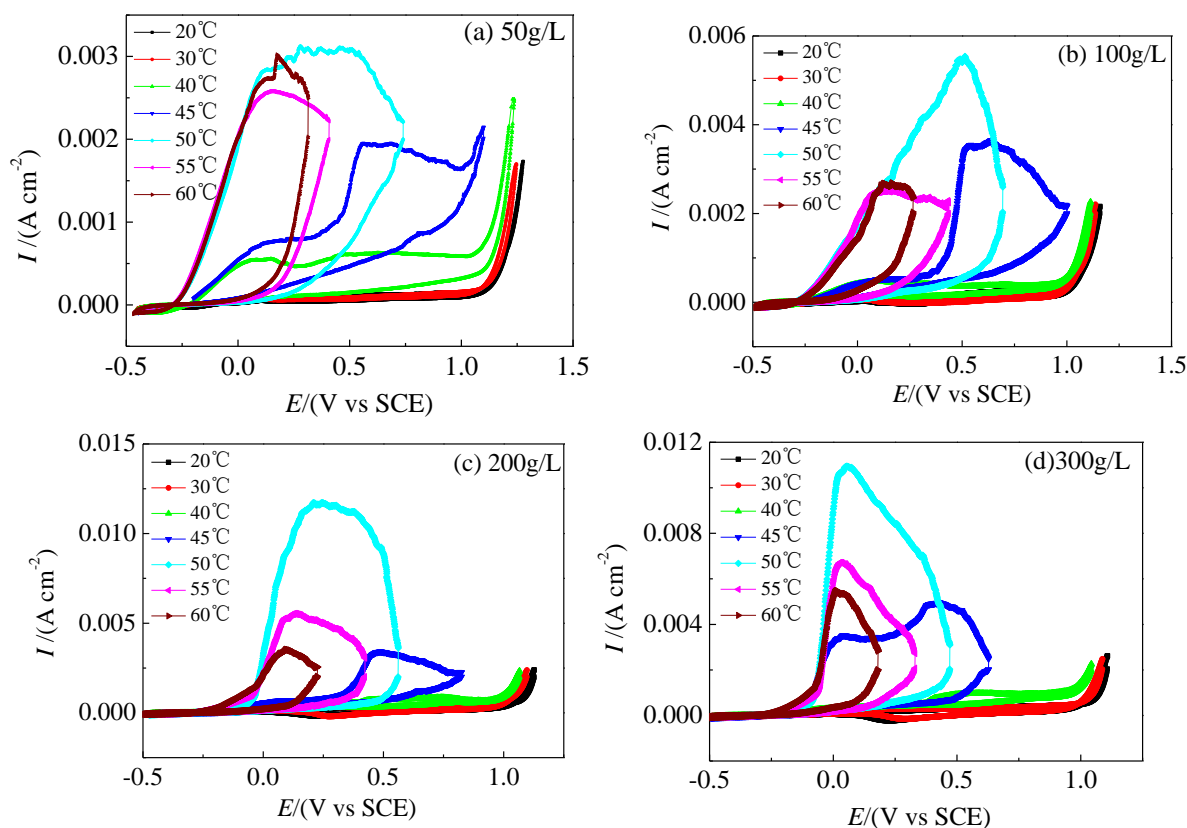
Figure 1. Cyclic voltammetry curves of 2205 DSS in various concentrations of NaCl solutions: (a) 50 g/L, (b) 100g/L, (c) 200 g/L, (d) 300 g/L at different temperatures.

Figure 1 shows the cyclic voltammetry curves of 2205 DSS in different concentrations of NaCl solutions under different temperatures. It can be seen that the current density increases slowly with the increase of the polarization potential, but when the polarization potential reaches a specific value, the current density begins to increase significantly, indicating that the passive film on the surface of 2205 DSS was broken, and this potential was defined as the breakdown potential (E_b). When the temperature is below 40 ℃, breakdown potential shifts to negative, but the displacement is very small, and it can be seen that the polarization curves of forward and backward potentiodynamic scans are almost coincident with negligible hysteresis loop, which indicates the transpassivity characteristic of passivation breakdown [18]. However, when the temperature is above 45 ℃, the breakdown potential drops significantly with increasing temperature, and the cyclic voltammetry curves of 2205 DSS exhibits a large hysteresis loop, suggesting that the repassivation of existing pits becomes difficult, it means the occurrence of pitting [18].
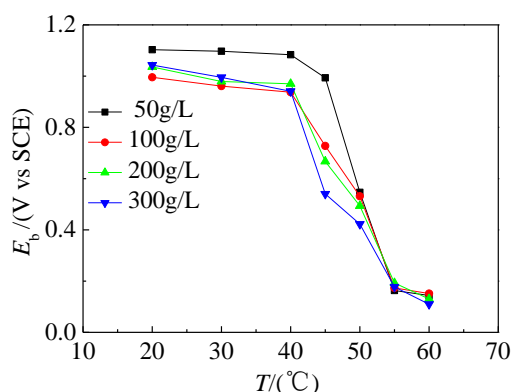
Figure 2. The breakdown potential of 2205 DSS in various concentrations of NaCl solutions at different temperatures.

Figure 2 shows that the breakdown potential of 2205 DSS in different concentrations of NaCl solutions, demonstrating the same tendency to change with rising temperature. It can be clearly seen that there is a significant decrease in the breakdown potential of 2205 DSS when the temperature increases from 40 ℃ to 45 ℃. Szklaska [24] thinks that as the temperature increases, chloride adsorption on the metal surface becomes stronger and the pitting potential tends to be smaller. However, according to Figure 1 and Figure 2, it can be considered that the concentration of NaCl solution has little effect on the CPT of 2205 DSS, which is always within the range of 40~45 ℃.

3.2 Potentiostatic measurements

Figure 3(a) presents the result of potentiostatic measurements of 2205 DSS in different concentrations of NaCl solutions. It is clear that the current density increases with the increase of concentration of NaCl under the same temperature. At the same NaCl concentration, the current density is only slowly increasing in the initial stage, until the temperature is near or over 40 ℃ the current density begins to increase obviously. The temperature corresponding to a significant change in the current density is considered as the CPT [25], the determining method of CPT is given in Figure

3(b), and the results are listed in Table 2. It is clear that the values of CPT of 2205 DSS decrease with the increase of the concentration of NaCl solution, which may be caused by that the adsorption of Cl⁻ on the steel surface. The adsorption of Cl⁻ could increase with the increase of the salt concentration, resulting in the more difficulty for oxygen to reach the surface of 2205 DSS, thus promoting the pitting corrosion [23,26-28]. But, the difference is not remarkable, all the CPT are located in the temperature range of 40~45 °C. This is in agreement with the test results of cyclic voltammetry.
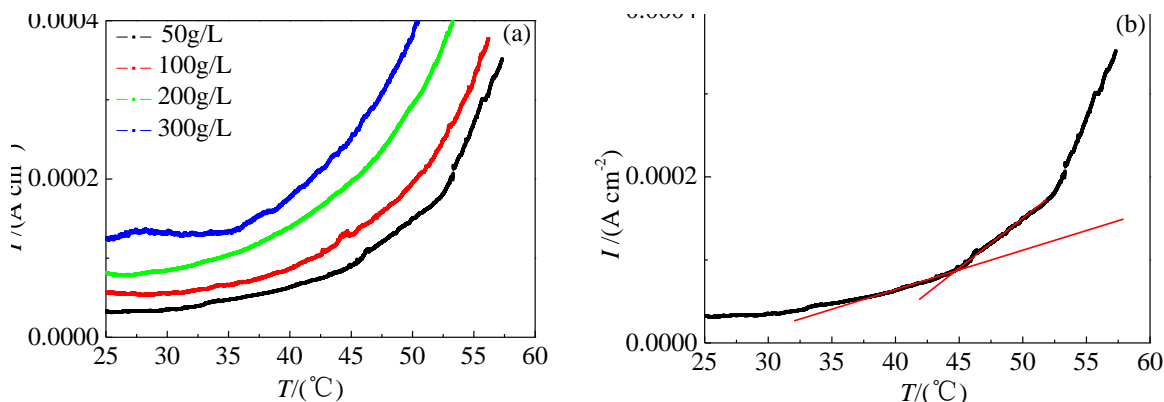
Figure 3. Potentiostatic polarization curves of 2205 DSS in various concentrations of NaCl solutions.

In addition, the CPT of 2205 DSS measured in the study is compared with that reported in literature [29-31], and the related data are listed in Table 3. It can be seen that the value of CPT in the literature is slightly higher than the measured value of this study, which is mainly due to the higher concentration of NaCl in the work, the data in Table 2 and Table 3 indicate that the increase in NaCl concentration lead to the decrease of CPT. It is also noted that the CPT value measured by potentiostatic technique is higher than that obtained through potentiodynamic polarization, this is in agreement with the results of this study.

Table 2. CPT of 2205 DSS in various concentrations of NaCl solutions.

C(g/L)	50	100	200	300
CPT(°C)	44.8	43.8	42.9	41.5

Table 3. Critical pitting temperature of 2205 DSS reported in the literature

Medium	Test methods	CPT	Reference
0.6 M NaCl	potentiodynamic polarization	45℃~55℃	[29]
0.6 M NaCl	potentiostatic	53℃	[29]
0.1 M NaCl	potentiodynamic polarization	45℃~55℃	[30]
0.1 M NaCl	Potentiostatic	59℃	[30]
0.1 M NaCl	potentiodynamic polarization	55℃~65℃	[31]
0.1 M NaCl	potentiostatic	73℃	[31]

3.3 Potentiodynamic polarization

In order to further understand the effect of temperature on the corrosion behavior of 2205 DSS in a series of NaCl solutions with different concentrations, the polarization curves of 2205 DSS in the NaCl solutions at two specific temperatures of 30 ℃ (below CPT) and 70 ℃ (above CPT) were measured and presented in Figure 4. The anodic polarization curve in Figure 4(a) shows that the current density increases with adding the polarization potential. At the temperature of 30 ℃, the current density is still small and is not enough to break the passivation film on the surface of 2205 DSS at low polarization potentials within a short immersing time. The similar results were also observed at 70 °C as shown in Figure 4(b), except that in the 300g/L NaCl solution. When the potential is about -0.05 V, the current density of 2205 DSS in 300 g/L NaCl solution increases significantly with increasing polarization potential, which means the occurrence of pitting corrosion, and also indicates the increase of temperature and NaCl concentration promotes the pitting corrosion of 2205 DSS. It also can be seen that the polarization curves shift toward the negative potential with increasing NaCl concentration.
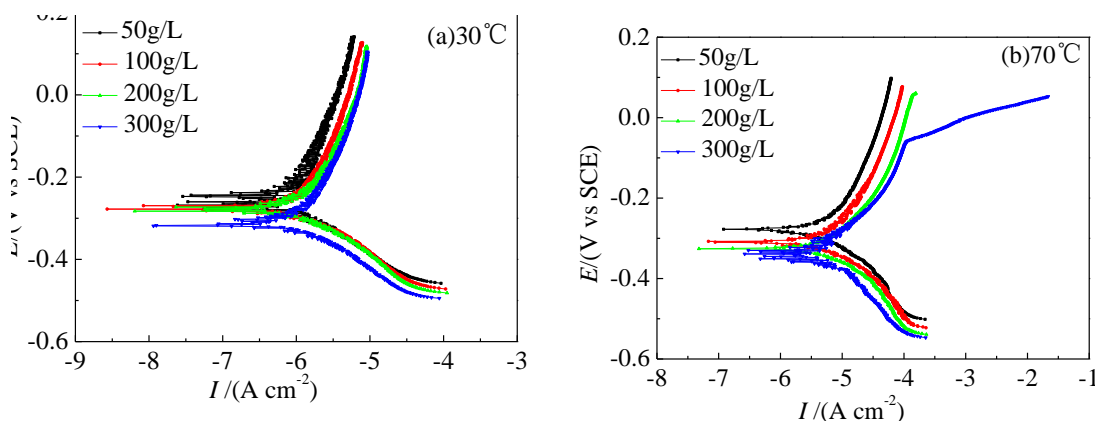
Figure 4. Polarization curves of 2205 DSS in various concentrations of NaCl solutions at 30 ℃ (a) and 70 ℃ (b).

Table 4. Electrochemical parameters of 2205 DSS in various concentrations of NaCl solutions at 30 ℃ and 70 ℃.

$T(℃)$	$C(g/L)$	$\beta_a(mV)$	$-\beta_c(mV)$	$I_{corr}(mA\ cm^{-2})$	$E_{corr}(V\ vs\ SCE)$
	50	507	124	1.1	-0.259
	100	494	139	1.5	-0.264
30	200	473	146	1.7	-0.271
	300	472	151	1.8	-0.301
	50	415	188	10.5	-0.277
	100	396	185	11.5	-0.309
70	200	334	193	12.8	-0.326
	300	317	209	13.3	-0.358

The corrosion current density (I_{corr}), corrosion potential (E_{corr}) cathode slope (β_c) and anode slope (β_a) obtained from polarization curves are listed in Table 4. These results presented that the corrosion current density increased but corrosion potential decreased with increasing concentration of NaCl, and, it is noted that the increase of temperature makes the corrosion current density increase obviously. With the increase of the NaCl solution concentration, the slopes of the cathode and the anode did not change much, which suggests the concentration has no obvious effect on the reaction mechanism of 2205 DSS in NaCl solution.

3.4 Electrochemical impedance spectroscopy

Electrochemical impedance spectroscopy is another helpful and effective methods for evaluating the corrosion behaivior of metals [32]. Nyquist plots of 2205 DSS in different concentrations of NaCl solutions were represented in Figure 5. It shows that the electrochemical impedance spectroscopy of 2205 DSS in NaCl solution exhibits a quarter circle at 30 ℃, while a diffusion tail appears at low frequencies at 70 ℃, which means that the diffusion reaction has taken place on the 2205 DSS electrode [33]. The equivalent circuit fitting the electrochemical impedance is shown in Figure 6, where, R_s is the solution resistance, R_p is the polarization resistance, CPE is the constant phase element which is often used to replace capacitance to give a more accurate fit to the impedance data [34], and W represents warburg impedance. The impedance parameters are listed in Table 5.
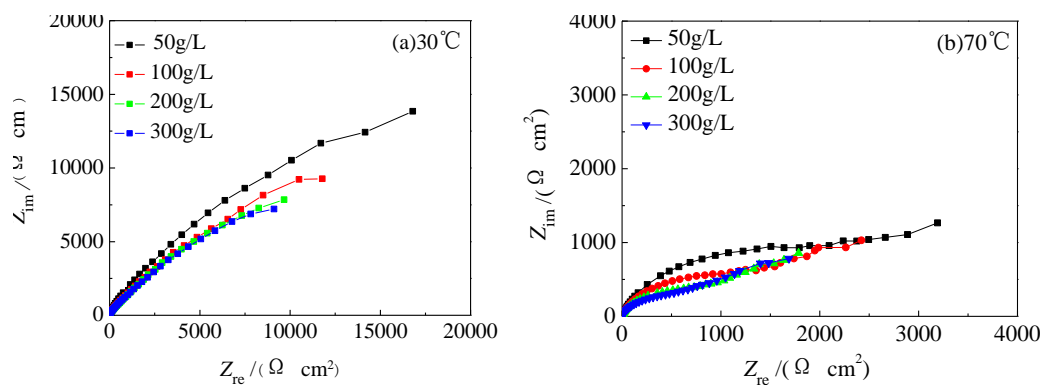
Figure 5. EIS of 2205 DSS in various concentrations of NaCl solutions at 30 ℃ (a) and 70 ℃(b).

Figure 6. Equivalent circuit for EIS of 2205 DSS in test solutions at 30 °C (a) and 70 °C (b).

As it shows, the values of R_p decrease with increasing NaCl concentration, and its value is significantly affected by temperature. For instance, in the NaCl aqueous solution of 50 g/L, the value

of R_p at 30 ^oC is about 28 times as high as that at 70 ^oC. While the increase in CPE is likely due to an increase in the local dielectric constant and a decrease in the thickness of a protective layer at the electrode surface, which would therefore reduce the corrosion resistance of the 2205 DSS in NaCl solution [35].

Table 5. Electrochemical impedance parameters of 2205 DSS in various concentrations of NaCl solutions at 30 ℃ and 70 ℃.

$T(℃)$	$C(\text{g L})$	$R_s(\Omega \text{ cm}^2)$	$CPE(\mu\text{F cm}^{-2})$	n	$R_p(\text{k}\Omega \text{ cm}^2)$	$W(\Omega \text{ cm}^{-2} \text{ S}^{-1})$
	50	3.1	193	0.82	24.8	
30	100	1.6	231	0.80	17.0	
	200	1.1	273	0.78	14.6	
	300	1.0	289	0.79	13.2	
	50	1.5	262	0.83	1.9	0.002069
70	100	0.9	223	0.84	1.1	0.002215
	200	0.6	244	0.85	0.7	0.002645
	300	0.7	269	0.83	0.5	0.002623

3.5. SEM examination

In order to ensure the effect of temperature on the corrosion of 2205 DSS in NaCl solution, SEM morphologies of 2205 DSS after immersed in 300 g/L NaCl solution for 7 days at 30 ℃ (a) and 70 ℃ (b) are given in Figure 7. It is clear that the surface of 2205 DSS immersed at 30 ℃ is much less damaged, only very weak pitting phenomenon can be observed at the defect of the specimen surface. However, when at 70 ℃, the passivation film of 2205 DSS surface had been broken and a large and deep pitting hole was formed. The results further reflect the effect of temperature on the corrosion behavior of 2205 DSS in NaCl solution.
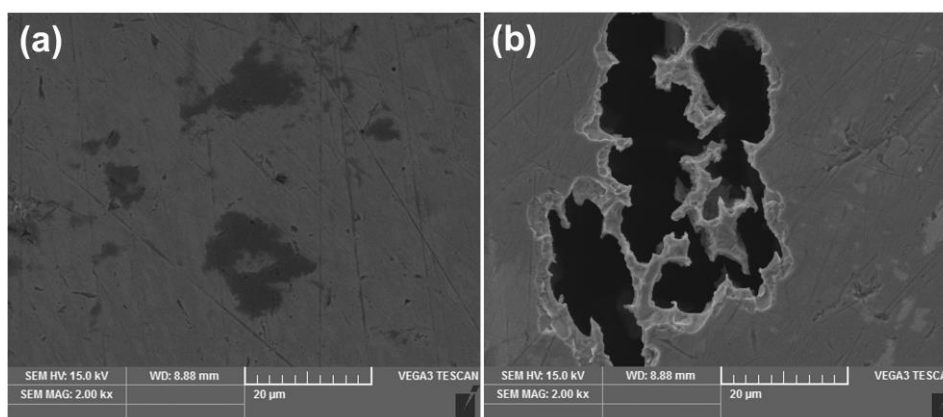
Figure 7. SEM morphologies of 2205 DSS after immersed in 300 g/L NaCl solution for 7 days at 30 °C (a) and 70 °C (b).

4. CONCLUSIONS

The critical pitting temperature of 2205 DSS in studied NaCl solution is located in the temperature range of 40~45 ℃ and slightly decreases with the increase of the concentration of NaCl solution. The corrosion current density increases but corrosion potential and polarization resistance decrease with increasing concentration of NaCl, and temperature can significantly affect the corrosion of 2205 DSS in NaCl solution.

References

1. F. Hengsbach, P. Koppa, K. Duschik, M.J. Holzweissig, M. Burns, J. NellesenW. Tillmann, T. Tröster, K.-P. Hoyer and M. Schaper, *Mater. Design.*,133 (2017) 136.
2. J. Wan, H. Ruan, J. Wang and S. Shi, *Mater. Sci. Eng*. A, 711 (2018) 571.
3. I.N. Bastos, S.S. M. Tavares, F. Dalard and R. P. Nogueira, *Scripta. Mater.*, 57 (2007) 913.
4. M.A. Makhdoom, A. Ahmad, M. Kamran, K. Abid and W. Haider, *Surf. Interface*., 9 (2017) 189.
5. R. Silverstein, D. Eliezer and B. Glam, *Energy. Procedia.*, 107 (2017) 199.
6. F. Iacoviello, V.D. Cocco and L. D.Agostino, *Structural. Integrity. Procedia.*, 3 (2017) 276.
7. A.P. Tschiptschin, L.B. Varela, C.E. Pinedo, X.Y. Li and H. Dong, *Surf. Coat. Tech.,* 327 (2017) 83.
8. R.T. Loto and J. Mater. Res. Technol, *J. Mater. Sci. Technol.,* 6 (2017) 203.
9. G. Chail and P. Kangas, *Procedia. Structural. Integrity*., 2 (2016) 1755.
10. L. Wickström, K. Mingard, G. Hinds and A. Turnbull, *Corros. Sci.*, 109 (2016) 86.
11. L.Q. Guo, Y. Bai, B.Z. Xu, W. Pan, J.X. Li and L.J. Qiao, *Corros. Sci.*, 70 (2013) 140.
12. Y. Zuo, H. Wang, J. Zhao and J. Xiong, *Corros. Sci.*, 44 (2002) 13.
13. J. Soltis, *Corros. Sci.*, 90 (2015) 5.
14. V. Vignal, H. Zhang, O. Delrue, O. Heintz, I. Popa and J. Peultier, *Corros. Sci.*, 53 (2011) 894.
15. L. Peguet, A. Gaugain, C. Dussart, B. Malki and B. Baroux, *Corros. Sci.*, 60 (2012) 280.
16. B. Deng, Y. Jiang, J. Gong, C. Zhong, J. Gao and J. Li, *Electrochim. Acta.*, 53 (2008) 5220.
17. S.-H. Jeon, S.-T. Kim, I.-S. Lee and Y.-S. Park, *Corros. Sci.*, 52 (2010) 3537.
18. F. Eghbali, M.H. Moayed, A. Davoodi and N. Ebrahimi, *Corros. Sci.*, 53 (2011) 513.
19. H. Luo, X.G. Li, C.F. Dong and K. Xiao, *Arab. J. Chem.*, 10 (2017) S90.
20. B. Wei, Z.Q. Bai, C.X. Yin and W.W. Li, *Transactions of Mate. Heat. Treatment*, 30 (2009) 73.
21. M. Naghizadeh and M.H. Moayed, *Corros. Sci.*, 94 (2015) 179.
22. H. Farnoush, A. Momeni, K. Dehghani, J.A. Mohandesi and H. Keshmiri, *Mater. Design.*, 31 (2010) 220.
23. E.A.A.E. Meguid and A.A.A.E. Latif, *Corros. Sci.*, 49 (2007) 263.
24. Szklarska-Smialowska, *Corrosion* 30 (1974) 161.
25. M. Hoseinpoor, M. Momeni, M.H. Moayed and A. Davoodi, *Corros. Sci.*, 80 (2014) 197.
26. P. Ernst and R.C. Newman, *Corros. Sci.*, 44 (2002) 943.
27. Chaofang. Dong, Hong. Luo, Kui. Xiao, Ting. Sun, Qian. Liu and Xiaogang. Li, *Journal of Wuhan University of Technology-Mater. Sci. Ed*. 26 (2011) 641.
28. N. Ebrahimi, M. Momeni, A. Kosari, M. Zakeri and M.H. Moayed, *Corros .Sci.*, 59 (2012) 96.
29. M. Zakeri and M.H. Moayed, *Corros Sci*, 85 (2014) 222.

30. N. Ebrahimi, M.H. Moayed and A. Davoodi, *Corros Sci*, 53 (2011) 1278.
31. F. Eghbali, M.H. Moayed, A. Davoodi and N. Ebrahimi, *Corros Sci*, 53 (2011) 513.
32. Z. Brytan, J. Niagaj and L. Reiman, *Appl. Surf. Sci*., 388 (2016) 160.
33. T. Hong and M. Nagumo, *Corros. Sci.*, 39 (1997) 961.
34. X. Zheng, S. Zhang and W. Li, *Corros. Sci.*, 80 (2014) 383.
35. N. Soltani, N. Tavakkoli, M.K. Kashani, A. Mosavizadeh, E.E. Oguzie and M.R. Jalali, *J. Ind. Eng. Chem.*, 20 (2014) 3217.